EXPERIMENTAL INVESTIGATION OF INFLUENCE OF INLET FLOW CONDITIONS ON SWIRLING FLOW GENERATED IN A THREE-DIMENSIONALLY CONNECTED DUAL ELBOW

T. Kubo[1,c], S. Ebara[1], H. Hashizume[1]

[1]Tohoku University, 6-6-01-2, Aramaki-aza-aoba, Aoba-ku, Sendai, Miyagi 980-8579, Japan

[c]Corresponding author: Tel.: +81227957906; Fax: +81227957906; Email: tkubo@karma.qse.tohoku.ac.jp

KEYWORDS:
Main subjects: flow visualization
Visualization method(s): a matched refractive-index PIV
Other keywords: inlet flow condition, FAC, secondary flow

ABSTRACT: Since it was reported that Flow-Accelerated Corrosion was largely influenced by a swirling flow, swirling flows formed in a dual elbow piping are scrutinized in this paper. The inlet flow condition of the piping is varied as an important parameter, and fully developed turbulent flow and four types of biased flow are used. In this study, a flow experiment using 2D-PIV measurement is conducted to evaluate the swirling flow generated downstream of the dual elbow. A test section consists of two acrylic 90-degrees elbows, connected three-dimensionally to each other, whose ratio of the curvature radius to a pipe inner diameter is 1.5. From the experimental results, it is confirmed that the flow condition at the outlet of the dual elbow is drastically changed according to the inlet flow conditions. A swirling flow which has local high velocity near the pipe wall is generated for all inlet conditions. However, the strength of the swirling flow which is represented by swirl number and its change along with the flow direction downstream of the dual elbow depends largely on the inlet conditions. It seems that high velocity region formed in the first elbow and vorticity in the direction of the pipe axis downstream of the dual elbow observed in the first elbow are very influential factors to determine the behavior of the swirling flow generated downstream of the dual elbow.

1. INTRODUCTION

One of the problems in aging nuclear or thermal power plants is the pipe wall thinning caused by Flow-Accelerated Corrosion (FAC) [1]. The FAC is recognized as one of the major factors in the pipe wall thinning. It occurs in complex flow fields which appear in and downstream of an elbow or downstream of an orifice, and affects a relatively wide range on pipe wall. The FAC depends on flow conditions and environmental ones, such as pH and temperature of flowing water. In addition, it has been reported that an asymmetrical pipe wall thinning due to the FAC occurred in an nuclear power plant and a swirling flow was estimated as its cause [2][3]. It is well known that swirling flows are often generated in pipings composed of a number of curved pipe elements, and occur in the three-dimensional layout of elbows. However, it is not clearly elucidated what the swirling flow generated is like and how it decays as flowing downstream through the piping. In the previous study, a swirling flow which occurred in a dual elbow with three-dimensional layout shown in Fig. 1 was experimentally evaluated using fully developed pipe turbulence as the inlet condition [4]. In the case, it was clarified that a swirling flow whose axis was eccentric shown in Fig. 2 was generated downstream of the dual elbow and that the swirling flow did not appear in terms of time-averaged velocity field when a straight pipe was inserted between the elbows. However, it is not well known that how the inlet condition affects the generation of the swirling flow in the piping. Therefore, in order to evaluate how the inlet flow conditions influence to generation and attenuation of the swirling flow generated downstream of a three-dimensional dual elbow, a flow experiment with 2D-PIV measurement is conducted by means of a refractive-index matching fluid. Obtained experimental data are discussed mainly in terms of time-averaged and fluctuating velocity in each visualized cross-section.

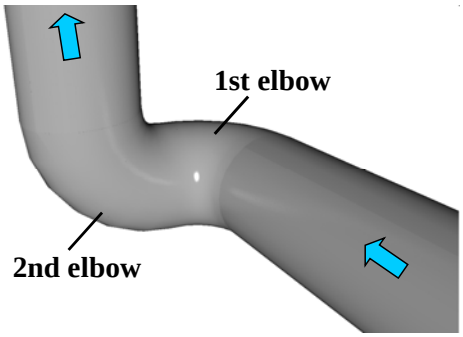

Fig. 1 Schematic of three-dimensionally connected dual elbow [4]

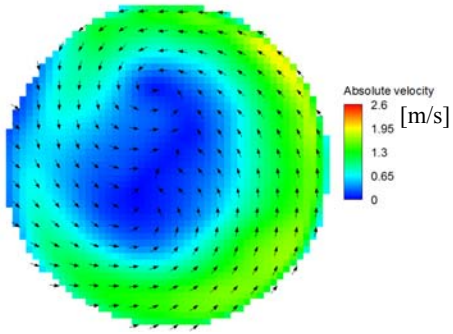

Fig. 2 A swirling flow formed 1D downstream of the outlet of the second elbow in the case of fully-developed turbulent flow [4]

2. EXPERIMENTAL METHODS AND CONDITION

The experimental apparatus is shown in Fig. 3. A test section consists of two acrylic 90-degrees elbows whose ratio of the curvature radius to a pipe inner diameter, D = 56 mm, is 1.5. This curvature radius is ordinarily used for normal piping. They are three-dimensionally connected as shown in Fig. 1. Working fluid is sodium iodide solution because the refractive index of sodium iodide solution is adjusted to almost the same value as that of acrylic and the influence of refraction upon optical visualization of flow field can be negligible. The Reynolds number for this experiment is fixed at 300,000. A laser as a sheet light source has an output of 25 mJ and an infrared wavelength of 808 nm. By means of a digital high-speed camera, 2048 images (1024 serial vector data) are obtained per one shot. Tracer particles of 10μm in diameter are made of glass coated with silver. In order to evaluate a development process of the swirling flow and its attenuation, visualization cross-sections are selected as shown in Fig. 4. In this paper, a cross-section parallel to the mainstream is referred to as "flow cross-section" and that vertical to the mainstream is "pipe cross-section". The flow cross-sections in the first and second elbows are measured. A coordinate system shown in the right-hand-side of Fig. 4 is used to discuss the experimental results. In addition, the pipe cross-sections on the inlet of the first elbow, the inlet and outlet of the second elbow, 1D, 2D and 3D downstream of the outlet of the second elbow are also measured. In this study, the inlet flow conditions are fully developed turbulent flow and four types of biased flow. A baffle plate shown in Fig. 5 is put 12D upstream of the inlet of the dual elbow to generate the four biased flows. The four patterns are numbered such as the biased flow 1, 2, and so on. In the biased flow 1 and 2, flow velocity on the extrados and intrados side of the first elbow is high as shown in Fig. 6(a), respectively. In the biased flow 3 and 4, flow velocity on the bottom side and the upper side of the Fig. 4 is high as shown in Fig. 6(b), respectively. Figures 6 show the velocity profiles 5D upstream of the inlet of the dual elbow. The vertical axes show the flow velocities normalized by the mean flow velocity, U_m, and the horizontal axes show distances from the pipe wall normalized by the inner diameter.

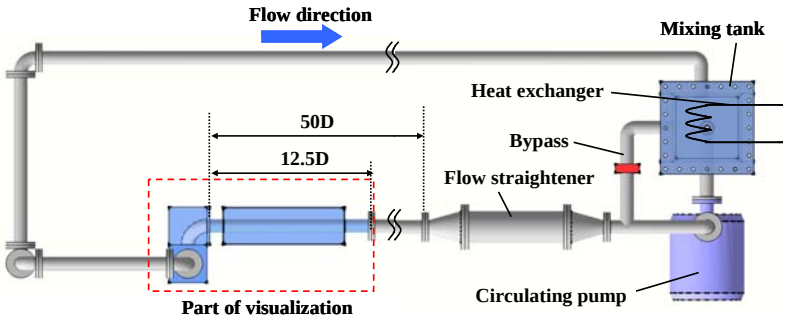

Fig. 3 Experimental apparatus

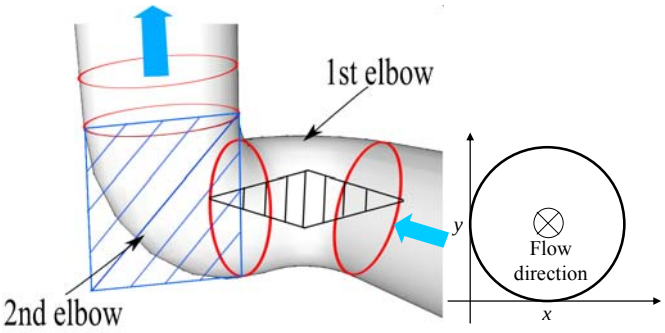

Fig. 4 Location of visualization areas and Coordinate system

Fig. 5 Baffle plate

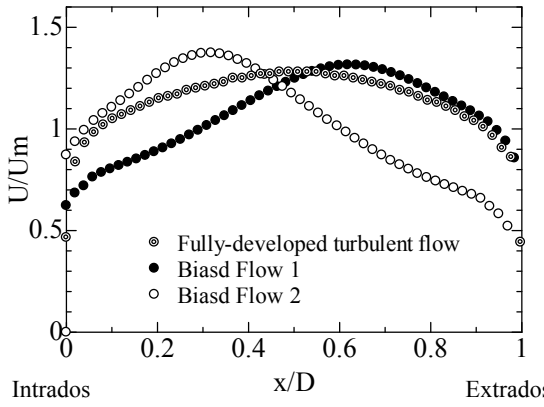

(a) Fully-developed turbulent flow and Biased flow 1 and 2

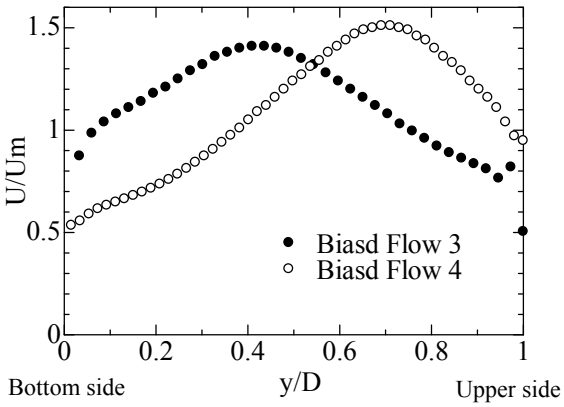

(b) Biased flow 3 and 4

Fig. 6 Flow distributions at the 5D (110 mm) upstream of the inlet of the dual elbow

RESULTS AND DISCUSSION

3.1 Swirling flows generated downstream of the dual elbow

Figures 7 show the time-averaged secondary flow fields 3D downstream of the dual elbow for all inlet conditions. From these figures, it can be seen a swirling flow having local high velocity near the pipe wall for all cases. In spite of the swirling flow generated, the flow conditions are different from each other except for the biased flow 3 and 4.

In this study, swirl number is adopted to represent the strength of the swirling flow. Its change in the direction of the pipe axis downstream of the dual elbow is shown in Fig. 8 for all inlet conditions. The swirl number is evaluated on the pipe cross-section and defined as follows [5].

$$S = \frac{G_\theta}{G_z \cdot R} \qquad \ldots(1)$$

where G_θ and G_z correspond to the angular momentum with respect to the pipe center and the moment in the axial direction, respectively, and R is the radius of the pipe. From Fig. 8, swirl numbers at the outlet of the dual elbow are higher in the case of the biased flow 1, 3 and 4 than the others and that in the case of the biased flow 2 is the smallest among all cases. The swirl number decreases monotonically as the flow goes downstream in the case of the biased flow 1 and 2 and that drastically decreases 1D downstream of the dual elbow in the case of the biased flow 3 and 4. The swirl number rises and falls but stays almost constant in the case of the fully developed turbulent flow. As shown in these figures, the inlet flow conditions largely affect the generation of the swirling flow and its attenuation. Hereafter, a discussion is made how the inlet flow conditions influence the formation of the swirling flow.

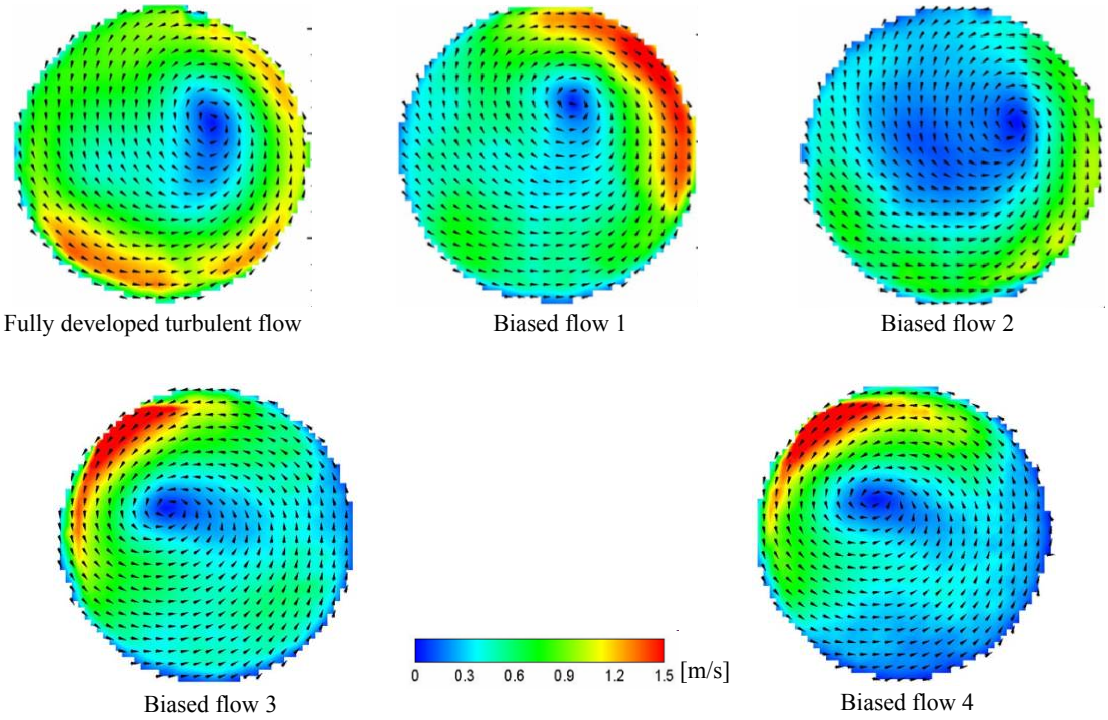

Fig. 7 Time-averaged secondary flow fields and velocity contours 3D downstream of the dual elbow

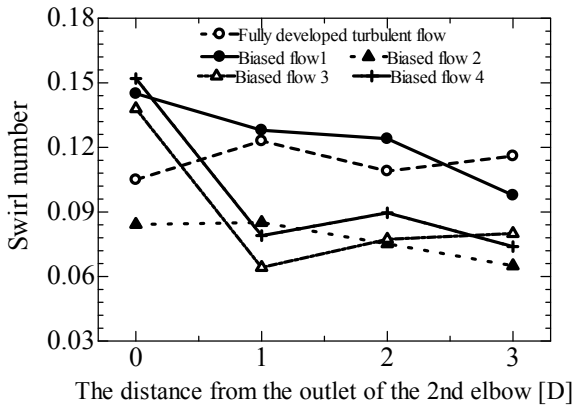

Fig. 8 Changes of swirl numbers downstream of the second elbow

3.2 Flow fields in the second elbow

Figures 9 show the time-averaged secondary flow fields at the outlet of the second elbow, in which the sides of A and B correspond to the intrados and extrados of the second elbow, respectively. It is found from Figs. 9 that the flow near the pipe wall swirls for all cases. However flows from the intrados to the pipe center are very different depending on the inlet flow conditions. In the case of the biased flow 1, 3 and 4, the flow is almost rectilinear. On the other hand, a clockwise flow appears in the case of the fully developed turbulent flow and the biased flow 2. In these cases, since there are circumferential flows in the opposite direction to each other, the swirl numbers become low. Moreover, in the case of the biased flow 1 and 4, the swirl numbers are particularly high due to high velocity area in the intrados of the second elbow.

The distributions of turbulent energy, defined as follows, at the outlet of the second elbow are shown in Figs. 10.

$$k = \frac{\frac{1}{2}\left(u'^2 + v'^2\right)}{\frac{1}{2}U_m^{\ 2}} \qquad ...(2)$$

where *u'* and *v'* correspond to the fluctuation components in the x and y directions, respectively. In the case of the fully developed turbulent flow and the biased flow 2, there can be seen large area where the turbulence energy is high as shown in Figs. 10. It can be considered because the clockwise and counterclockwise flows exist widely in the instantaneous field, and are mixed to generate large turbulent energy and small time-averaged velocity near the intrados of the elbow in these cases.

Figures 11 show time-averaged flow fields in the flow cross-section in the second elbow. For all cases, high velocity area appears in the intrados of the second elbow because of the effect of an elbow. However, the sizes of the high velocity area are different from each case. In the case of the biased flow 4, the width of the high velocity area is especially narrow and the flow velocity near the outlet of the second elbow is low. Figure 12 shows the velocity profiles in the flow cross-section at the outlet of the second elbow. The horizontal axis shows the distance from the pipe wall of the intrados normalized by the pipe inner diameter. In the case of the biased flow 4, the flow velocity in the intrados of the second elbow is low compared to the other cases as shown in Fig. 12 and it seems that this affects the large decrease in the swirl number between the outlet and 1D downstream of the second elbow as shown in Fig. 8. In the case of the biased flow 4, there is high velocity secondary flow in the intrados of the outlet of the second elbow as shown in Figs. 9. However, flow velocity in the intrados of the second elbow is low compared to the other cases as mentioned above. Therefore the high velocity secondary flow generated in the intrados at the outlet of the second elbow is not transported downstream and the swirl number 1D downstream of the second elbow becomes small. In the case of the biased flow 3, the flow velocity in the axis direction in the intrados at the outlet of the second elbow is high as shown in Figs 11, but the velocity in the secondary flow near the corresponding region is low. Thus the swirl number 1D downstream of the second elbow becomes small as well as the case of the biased flow 4. On the other hand, the swirl number does not attenuate in the case of the fully developed turbulent flow in spite that high secondary flow does not appear at the outlet of the second elbow. Hence more detailed measurement downstream of the dual elbow is necessary for more detailed understanding of the attenuation of the swirling flow.

Figures 13 show the distributions of turbulence energy in the flow cross-section in the second elbow. As shown in these figures, high turbulence energy areas appear near the center of the second elbow. It can be inferred that these areas are generated when the flow passing through the first elbow collides with the pipe wall of the second elbow.

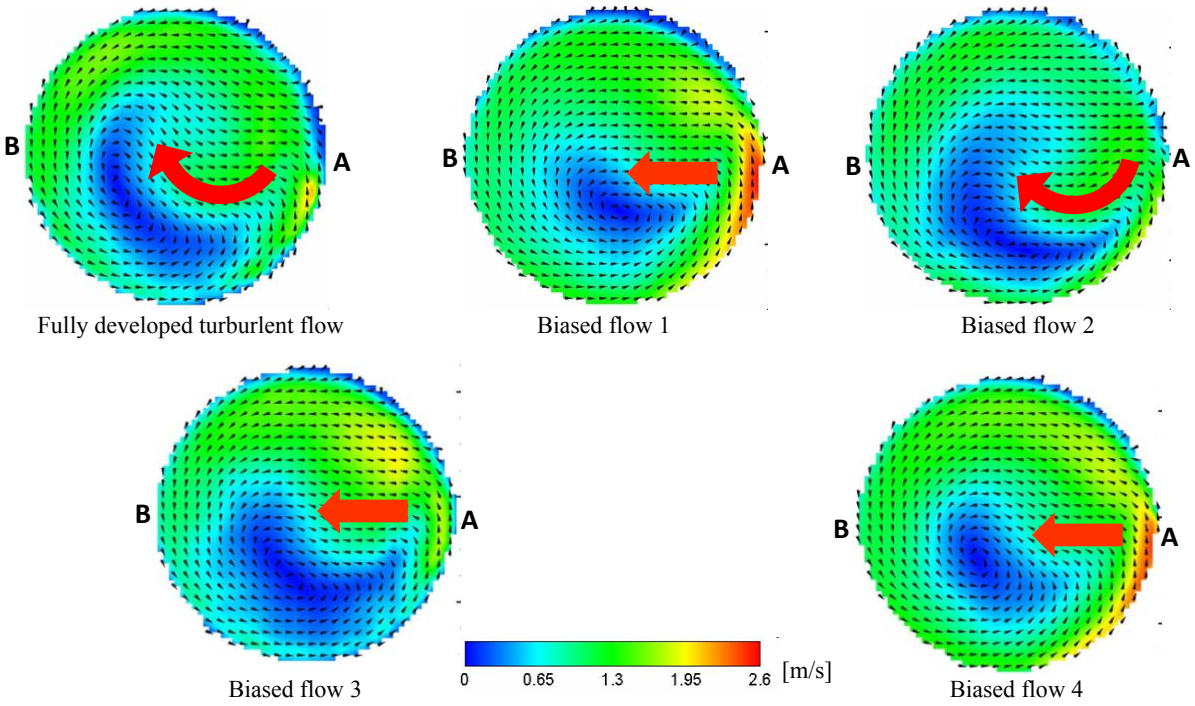

Fig. 9 time-averaged secondary flow fields and velocity contours at the outlet of the second elbow

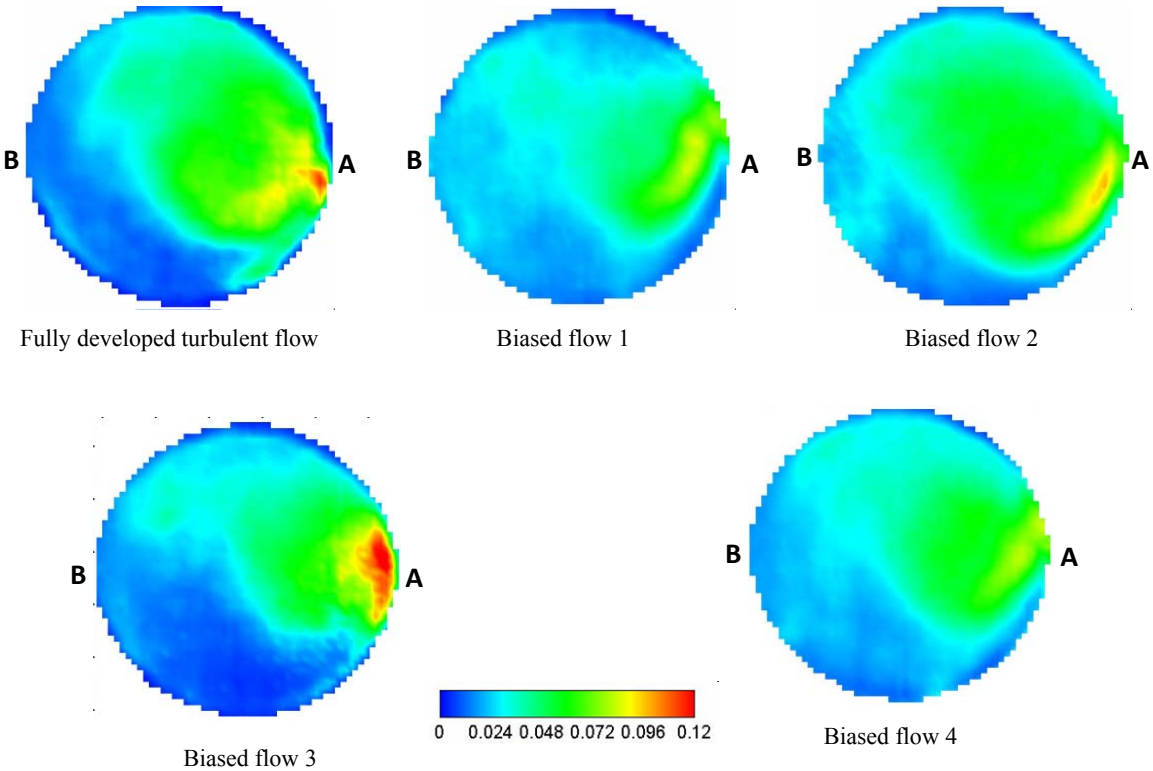

Fig. 10 Turbulence energy distributions at the outlet of the second elbow

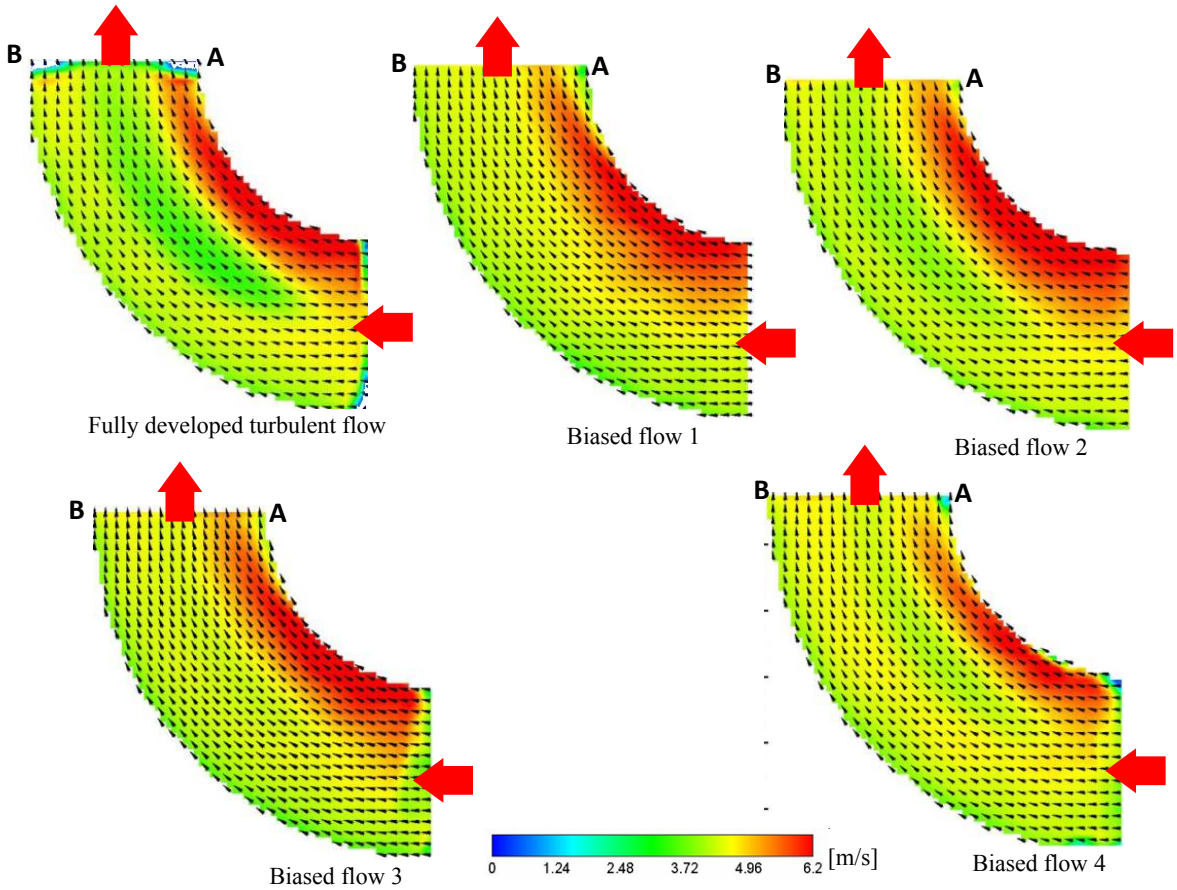

Fig. 11 Time-averaged flow fields in the flow cross-section of the second elbow

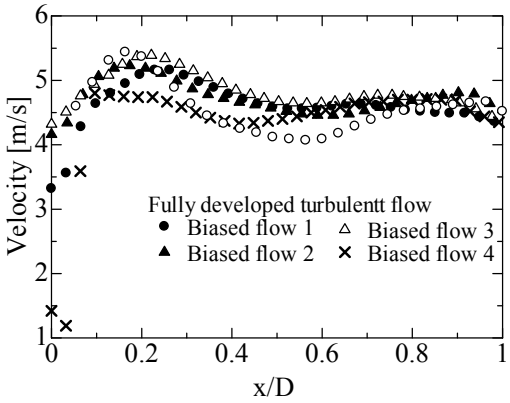

Fig. 12 Velocity distributions at the outlet of the second elbow

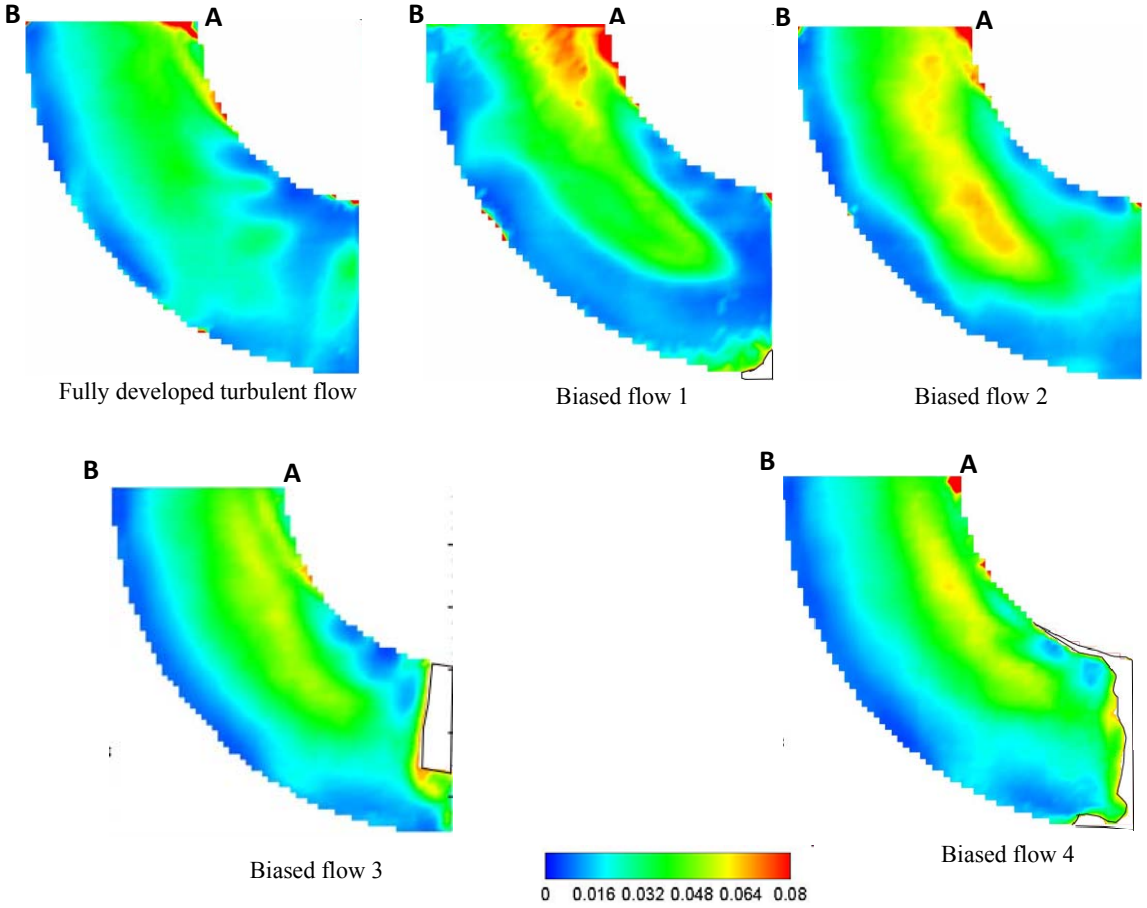

Fig. 13 Turbulence energy distributions in the flow cross-section of the second elbow

3.3 Flow fields in the first elbow

Figures 14 show time-averaged flow fields in the flow cross-section of the first elbow. High velocity areas appear in the intrados as well as the second elbow as shown in Figs.11, and the sizes of the high velocity areas are different from each case. Figures 15 and 16 show the velocity profiles in the flow cross-section at the inlet and outlet of the second elbow, respectively. The horizontal axes show the distances from the intrados wall of the first elbow normalized by the pipe inner diameter. In the case of the biased flow 2, flow velocity in the intrados of the inlet is high and that at the extrados is low. Moreover the flow velocity at the intrados of the outlet is low compared to the other cases as shown in Figs. 15 and 16. It can be considered because the high velocity area cannot curve along the intrados pipe wall and separates from it, then flows linearly into the center of the first elbow.

Besides, it seems that vorticity in the flow cross-section in the first elbow affects the generation of the swirling flow downstream of the dual elbow because the rotation direction of the vorticity is the same as that of the swirling flow

downstream of the dual elbow. Figures 17 show the vorticity distributions in the flow cross-section in the first elbow. In the case of the fully developed turbulent flow and the biased flow 2, negative area of vorticity is larger than the other cases. In the case of the biased flow 2, the vorticity is more likely to be negative because of the behavior of the high velocity area as mentioned above. This seems to be the cause that the swirling flow is less likely to occur in this case. On the other hand the negative areas of vorticity are small in the case of the biased flow 1, 3 and 4, so that the swirling flow is more likely to occur in the outlet of the second elbow compared to the fully developed turbulent flow and the biased flow 2.

Figures 18 show turbulence energy distributions in the flow cross-section of the first elbow. In the case of the fully developed turbulent flow, the turbulence energy is wholly lower than the other cases. It is because there is not the baffle plate for the biased flow, which is considered to act as a turbulent promoter. In the case of the biased flow 2, high turbulence energy area appears in the extrados of the first elbow. This is because the high velocity area passes through near the intrados and generates the high turbulence energy by colliding with the pipe wall on the extrados side of the first elbow.

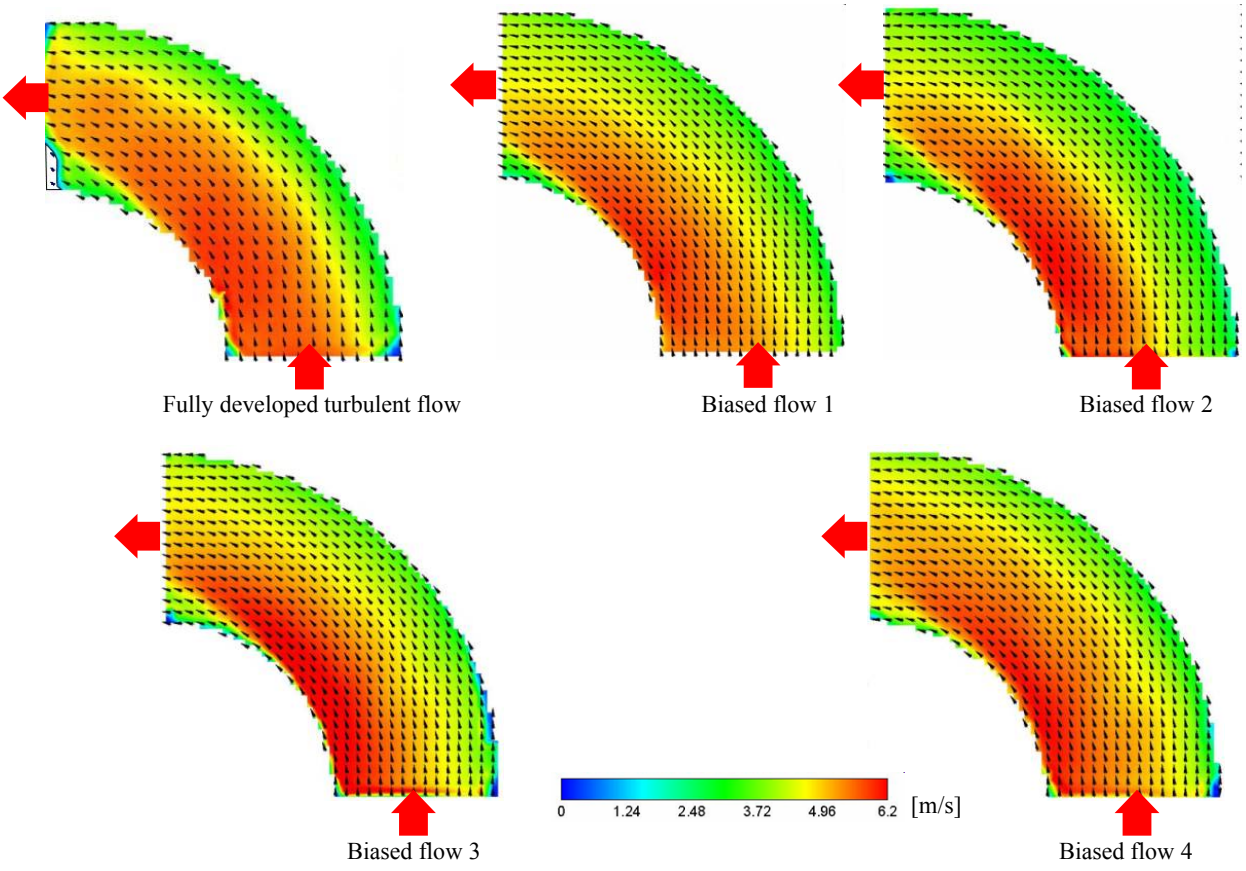

Fig. 14 Time-averaged flow fields in the flow cross-section of the first elbow

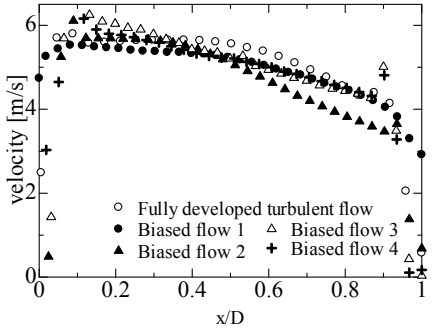

Fig. 15 Velocity profiles at the inlet of the first elbow

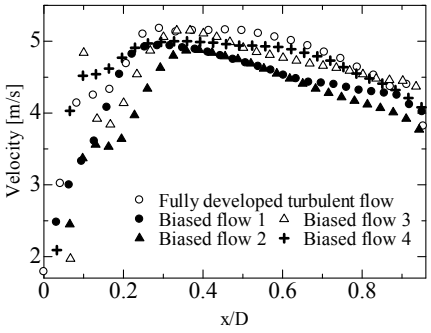

Fig. 16 Velocity profiles at the outlet of the first elbow

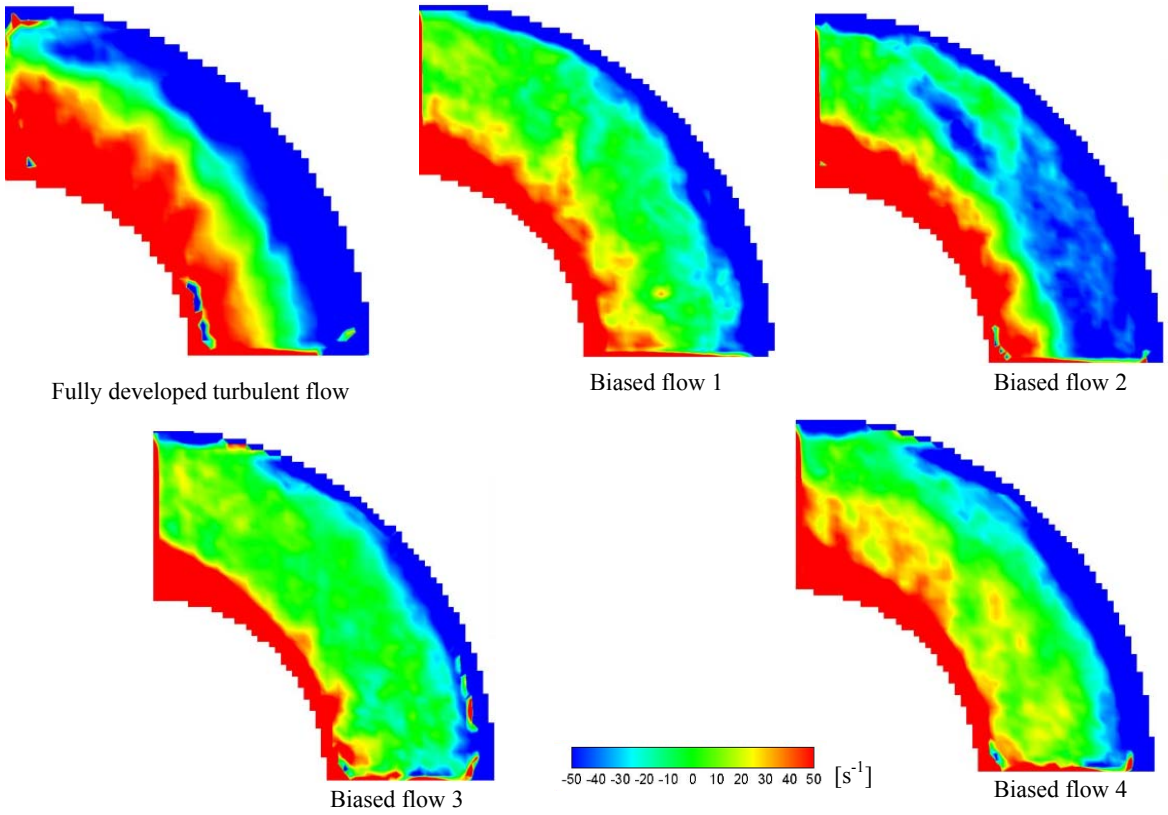

Fig. 17 Vorticity distributions in the flow cross-section of the first elbow

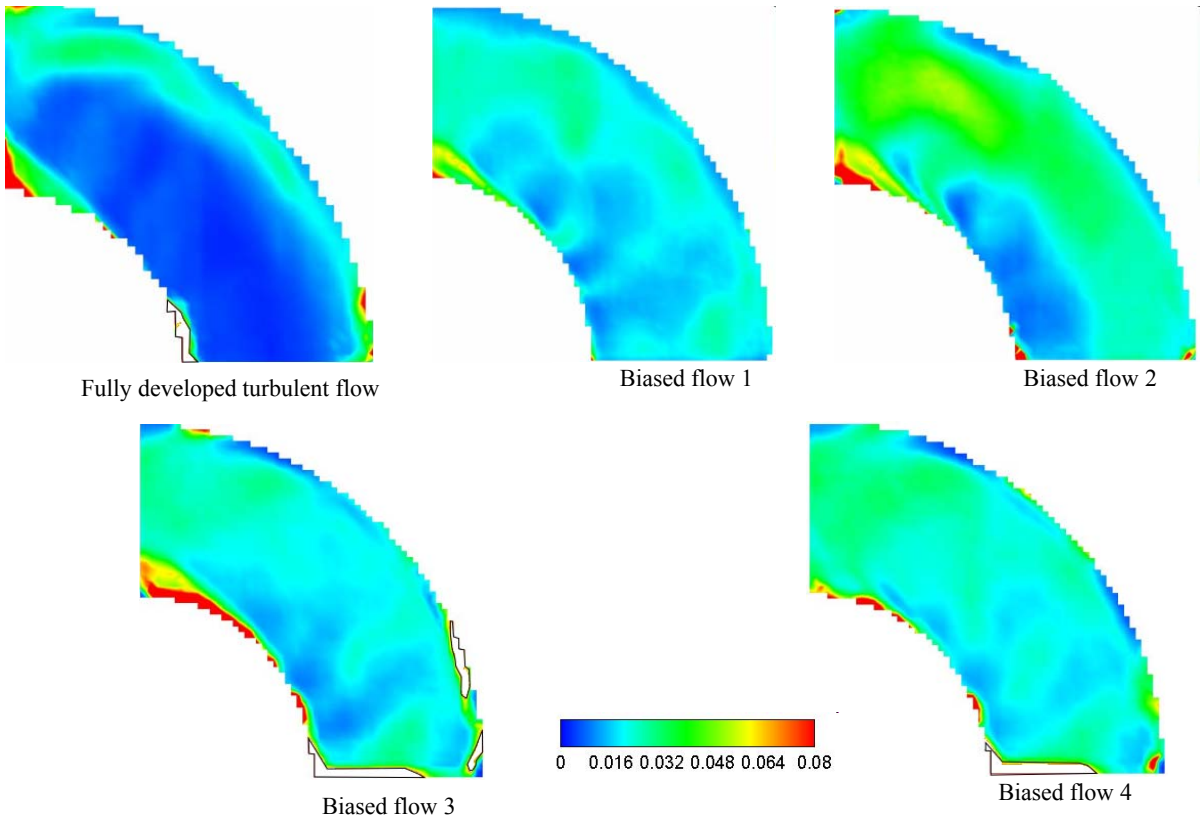

Fig. 18 Turbulence energy distributions in the flow cross-section of the first elbow

4. CONCLUTION

In this study, it is evaluated that how the inlet flow conditions influence to generation and attenuation of the swirling flow generated at the outlet of a three-dimensional dual elbow by using the matched refractive-index PIV measurement. As the inlet flow conditions, fully developed turbulent flow and four types of biased flow are applied. From the experimental results, swirling flow is generated for all cases. However, the characteristics of the swirling flows are different from each other. Swirl number is used as a parameter indicating the intensity of the swirling flow. In the case of the biased flow 1, the swirl number is high at the outlet of the dual elbow but it attenuates fast compared to the case of the fully developed turbulent flow. In the case of the biased flow 2, the swirl numbers at the outlet and downstream of the dual elbow stay lower level and the swirling flow is less likely to occur. It is attributed to high velocity region formed in the first elbow. In the case of the biased flow 3, the swirling number is high at the outlet of the second elbow and attenuates immediately 1D downstream of the second elbow. This arises from the flow condition that there is no high velocity area that exists in the case of the biased flow 1 in the intrados at the outlet of the second elbow due to the flattening of the flow velocity distribution. In the case of the biased flow 4, the swirling number is high at the outlet of the second elbow and attenuates drastically 1D downstream of the elbow as well as the case of the biased flow 3. It seems to affect the prompt attenuation of the swirling flow that the flow velocity in the pipe cross-section is small at the outlet of the intrados of the second elbow. In the case of the fully developed turbulent flow, the swirl number is relatively small and the turbulence energy is high at the outlet of the second elbow compared to the case of the biased flow 1, 3 and 4. However, the swirling flow is most prone to sustain downstream of the dual elbow. In addition, vorticity in the first elbow in the flow cross-section is important to investigate the characteristics of the swirling flow generated by the dual elbow.

REFERENCES

1. Dooley R.B. Chexal V.K. *Flow-accelerated corrosion of pressure vessels in fossil plants.* International Journal of Pressure and Piping, 77, P. 85-90 (2000)

2. Masashi KAMEYAMA . *Analysis of pipe wall Thinning Phenomenon in Secondary Pipe Rupture at Mihama Unit 3.* Proceedings of the Japan Society of Mechanical Engineers, Vol 8, p. 42-45 (2005)

3. Masakazu OHKUBO. et al. *Investigation on Pipe-Wall Thinning by Flow Accelerated Corrosion* (*Occurrence of Asymmetrical Flow by Combined Effect of Swirling Flow and Orifice Bias*). Transactions of the Japan Society of Mechanical Engineers (B), Vol. 77 (774), P. 386-394 (2011)

4. T. Kubo. H. Yanai. S. Ebara, H. Hashizume. *Experimental Estimation in Characteristics of Swirling Flow Appearing in a Three-Dimensionally Connected Dual Elbow Layout by Means of Matched Refractive-index PIV Measurement*. Proceedings of The 11th Asian Symposium on visualization, ASV11-po-30 (2011)

5. Katsumi AOKI. et al. *Study of the cylindrical combuster flow with swirling flow.* Transactions of the Japan Society of Mechanical Engineers B, Vol. 51 (468), P. 2759-2766 (1985)